Preliminary experiment on characterization of RANS-II neutron production via the ^{7}Li(p, n)^{7}Be reaction with 2.49 MeV proton injection

S. IZUMITANI[1], Y. IKEDA[2], T. KOBAYASHI[2], S. IKEDA[2], Y. WAKABAYASHI[2], K. FUJITA[2], K. SUGIHARA[1,2], N. SHIGYO[1], K. TANAKA[2], Y. OTAKE[2]

1 Kyushu University, Fukuoka, 819-0395, Japan

2 RIKEN, Wako, 351-0198, Japan

e-mail: shog0311@kune2a.nucl.kyushu-u.ac.jp

Experiments associated with the first measurement for neutron production characteristics via the ^{7}Li(p,n)^{7}Be reaction at RANS-II were performed by applying two methods of the long counter with ^{3}He gas counter and the foil activation technique using an indium foil. The experimental data in a form of reaction rate were compared with calculations by using PHITS code simulating the experimental condition. It was found there were overestimation in the calculation to some extent in both methods observed by comparison of calculation to experiment. We have investigated possible causes for the discrepancies between experiments and calculations. As the data of experiments and calculations were very preliminary and still underway to finalize credible comparisons, we report tentative analyses concerning p-Li neutron production cross section, change of proton beam position and profile on the Li target. Lastly we list up major source of concerning uncertainty and error to be clarified.

1 Introduction

To meet increasing demands for neutrons, RIKEN has been developed the proton accelerator based compact neutron source, called RANS (RIKEN Accelerator-driven compact Neutron Source) by using the ^{9}Be(p, n)^{9}B reaction with 7 MeV proton injection for the neutron production [1]. RANS comes up with successful achievements in several application fields demonstrating a promising potential capability of CANS (a Compact Accelerator-driven Neutorn Source) in expanding needs such as non-destructive diagnostic tool for infrastructure concrete media [1]. From the compactness point of view, accelerator and neutron production target are identified as key technological elements to be R&D items. RANS-II has been developed as a prototype of more realistic compact source by using the ^{7}Li(p, n)^{7}Be reaction, which produces neutrons by rather low energy proton incidence. RANS-II adopted this reaction with 2.49 MeV proton accelerator mainly because of compactness requirement. Although the cross section of this reaction has been studied for many years [2–8], there is still an issue to be confirmed as the compact neutron source performance; neutron production yield and angular distribution using a thick Li target configuration with intense proton beam injection. Thus, we started an experimental program to validate neutron characteristics in terms of neutron yield and angular distribution of RANS-II using the ^{7}Li(p, n)^{7}Be reaction as its accomplishment test of the system accepting the proton beam on the Li target.

The experimental data in a form of reaction rate were obtained using two detectors; a ^{3}He long counter which has a thick cylinder moderator, and indium activation foils for using ^{115}In(n, n$'$)^{115m}In reaction which has a low threshold energy of 336 keV. In this paper, we report the validity of calculations and the current status of evaluation through comparison with calculations by using PHITS-2.88 [9] simulating the experimental condition. Although the data of experiments and calculations were very preliminary, sources of concerning uncertainty and error were analyzed as much as possible.

2 Experiment

Two experiments were conducted to obtain reaction rates; (i) ^{3}He long counter and (ii) indium foil activation. Reasons for applying the two methods were as follows; TOF which is assumed to be the most efficient for the neutron spectrum measurement, is not effective at the RANS-II shown in **Figure 1**, because of a short flight path available and also a rather long proton pulse width. On the other hand, a proton recoil spectrometer is used for a measurement of an energetic neutron spectrum. However, there expected a large uncertainty in determining below 1 MeV neutron energy in this neutron production case of 2.49 MeV proton injection on lithium. Indium foils were preliminary used in expection of measuring several hundred keV neutrons because the ^{115}In(n, n′)^{115m}In reaction has a threshold of 336 keV. It is also an objective to be validate by this experiment.

(i) ^{3}He long counter

Configuration of ^{3}He long counter are shown in **Figure 2**. A LND 252295 ^{3}He counter was used. The applied voltage was 1600 V. The counter was put in a moderator composed of polyethylene cylinder and 0.3 cm thick 50 wt% B_4C gum. At first, Counting rates using a 3.6 MBq ^{252}Cf source were measured. The distances between the source and the detector were 100, 50, and 15 cm. After the measurement, counting rates with proton beams were measured. The distance from a Li target to the ^{3}He long counter was 288.7 cm. The proton beam currents were between 0.066 and 0.59 µA.

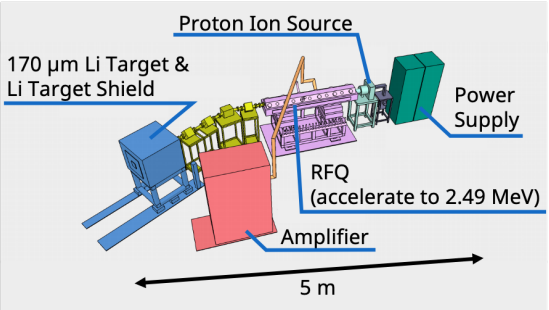

Figure 1 Configuration of RANS-II

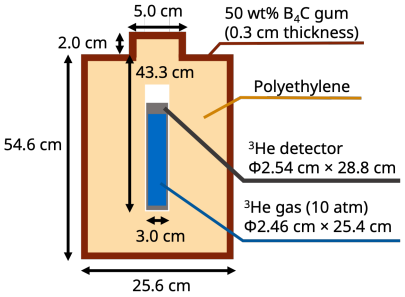

Figure 2 Configuration of ^{3}He long counter

(ii) Indium foil activation

The four indium foils (In#1 ~ In#4) were placed on a cardborad located 1.6 cm from the target. **Figure 3** shows arrangement of the foils. The size and weight of indium foils and distances from In#1 are shown in **Table 1**. The proton beam with an average current of 3.9 µA was irradiated for 15 minutes. After the irradiation, the foils were cooled and 336 keV γ-rays emitted from the ^{115}In(n, n′)^{115m}In reaction and 1293 keV γ-rays emitted from the ^{115}In(n, γ)^{116m}In reaction were measured by a HPGe detector. In#1 ~ In#3 were placed at 2.7 cm from the surface of the HPGe detector, and In#4 was placed at 0.20 cm from the surface. The relative efficiency of the HPGe detector is 10 %.

3 Simulation

Reaction rates were calculated using PHITS-2.88. ENDF-B/VII.0 [10] was used for the ^{7}Li(p, n) reaction. JENDL-4.0 [11] was used for neutron incident reactions. Proton beams with the diameter of 1.0 cm and uniform distribution were incident on the center of a Li target (diameter 5 cm, thickness 170 µm) to generate neutrons. The number of neutrons generated from the Li target was 1.21 × 10^{-4} [/proton].

(i) ^{3}He long counter

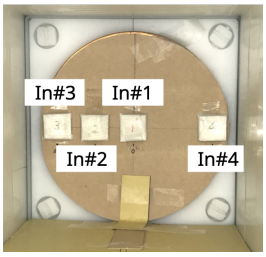

Figure 3 Experiment using indium foil activation

Table 1 Information of Indium

	Size [cm^3]	Weight [g]	Distance from In#1 [cm]
In#1	1.8 × 1.7 × 0.20	4.66	0
In#2	1.7 × 1.8 × 0.20	4.99	2.8
In#3	1.8 × 1.9 × 0.20	4.98	5.5
In#4	1.7 × 1.9 × 0.20	4.90	5.4

Figure 4 illustrates the comutational geometry using PHITS. Only the RANS-II target shield and the ^{3}He long counter were assumed because scattered neutrons from floors, walls, and roofs were considered to be negligible. Neutron track lengths in the ^{3}He was measured by a T-track tally. Neutron measurements emitted from a ^{252}Cf source were also performed. The energy spectrum shape defined by JIS Z 4521 [12] was applied in the simulation.

(ii) Indium foil activation

Figure 5 depicts the geometry of simulation. Indium foils were placed on the same positions as the experiment. Only RANS-II target shield and indium foils were assumed. Neutron track lengths in the foils were obtained by T-track tallies.

Reaction rates was calculated using the T-track results. In the calculations, JENDL-4.0 was used for the ^{3}He detector, and JENDL dosimetry file 99 [13] was used for the indium foil activation.

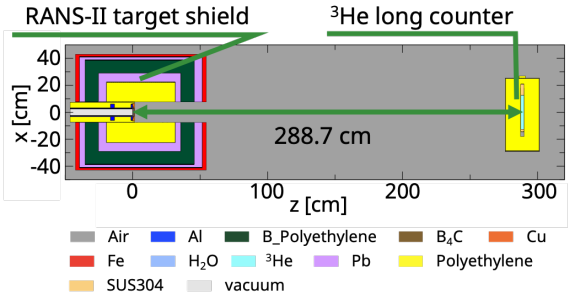

Figure 4 Geometry of calculation for the ^{3}He long counter

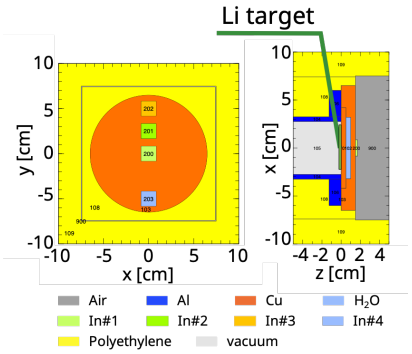

Figure 5 Geometry of calculation for the indium foil activation

4 Results and Discussion

(i) ^{3}He long counter

Table 2 shows the comparison of counting rates in the measurements using the ^{252}Cf source between the experiment and PHITS. Errors in the tables include statistical errors. The calculation to experiment (C/E) using the ^{252}Cf source was 1.76 ~ 1.90. It is attributed to uncertainties of the ^{3}He long counter of PHITS such as gas pressure and simension of sensitive area. For example, when pressure is 1 atm, calculation at 100 cm is 51.3 [/s], that is 41 % smaller than that for 10 atm. **Table 3** shows neutron yields on proton beams currents. For the proton beam measurements, C/E was 8.48 ~ 8.77. Therefore, PHITS overestimated the experimental values.

Table 2 Comparison of counting rates in the measurements using ^{252}Cf source

Distance [cm]	Exp. [/s]	PHITS [/s]	C/E
100	71.0 ± 0.73	125	1.76
50	260 ± 0.94	495	1.90
15	2317 ± 4.9	4264	1.84

Table 3 Comparison of the dependence of neutron yields on the proton beams

Current [μA]	Exp. [/s]	PHITS [/s]	C/E
0.066	217 ± 1.28	1842	8.48
0.085	278 ± 2.12	2379	8.56
0.10	329 ± 2.87	2884	8.77

(ii) Indium foil activation

Table 4 Comparison of the reaction rates for the ^{115}In(n, γ)^{116m}In reaction at 3.9 μA

	Exp. [/s]	PHITS [/s]	C/E
In#1	$(5.5 \pm 0.012) \times 10^{-17}$	2.3×10^{-16}	4.2
In#2	$(5.3 \pm 0.021) \times 10^{-17}$	1.8×10^{-16}	3.4
In#3	$(4.9 \pm 0.033) \times 10^{-17}$	1.8×10^{-16}	3.7
In#4	$(4.1 \pm 0.082) \times 10^{-17}$	1.8×10^{-16}	4.4

Table 5 Comparison of the reaction rates for the ^{115}In(n, n′)^{115m}In reaction at 3.9 μA

	Exp. [/s]	PHITS [/s]	C/E
In#1	$(5.5 \pm 0.12) \times 10^{-20}$	4.4×10^{-19}	8.0
In#2	$(3.4 \pm 0.10) \times 10^{-20}$	1.9×10^{-20}	0.56
In#3	$(1.6 \pm 0.17) \times 10^{-21}$	1.8×10^{-21}	1.1

Tables 4 and **5** show reaction rates of the ^{115}In(n, γ)^{116m}In reaction and the ^{115}In(n, n′)^{115m}In reaction, respectively. Errors in the table include statistical errors. For the the ^{115}In(n, γ)^{116m}In reaction, C/E was 3.4 ~ 4.4. On the other hand, the ^{115}In(n, n′)^{115m}In reaction, C/E was 0.56 ~ 8.0. One of the possible causes for the differences of C/E between the two reactions is that proton beam position between the experiment and the simulation is different. Neutrons from the ^{7}Li(p, n) reaction with at most 800 keV are easily slowed below 336 keV of the ^{115}In(n, n′)^{115m}In reaction threshold by the target shield. In addition, these neutrons tend to be emitted in forward direction. Therefore, reaction rates for different beam positions was calculated by PHITS.

Tables 6 and **7** show reaction rates of the ^{115}In(n, γ)^{116m}In and the ^{115}In(n, n′)^{115m}In reaction when position of the proton beam is moved 1.2 cm from In #1 to In #2, respectively. This result shows that the reaction rates for the ^{115}In(n, n′)^{115m}In reaction largely depends on the proton beam position.

Table 6 Comparison of the reaction rates for ^{115}In(n, γ)^{116m}In reaction at 3.9 μA when the position of the proton beam is moved 1.2 cm from In #1 to In #2

	Exp. [/s]	PHITS [/s]	C/E
In#1	$(5.5 \pm 0.012) \times 10^{-17}$	2.2×10^{-16}	4.0
In#2	$(5.3 \pm 0.021) \times 10^{-17}$	2.0×10^{-16}	3.8
In#3	$(4.9 \pm 0.033) \times 10^{-17}$	1.8×10^{-16}	3.7
In#4	$(4.1 \pm 0.082) \times 10^{-17}$	1.6×10^{-16}	3.9

Table 7 Comparison of the reaction rates for ^{115}In(n, n′)^{115m}In reaction at 3.9 μA when the position of the proton beam is moved 1.2 cm from In #1 to In #2

	Exp. [/s]	PHITS [/s]	C/E
In#1	$(5.5 \pm 0.12) \times 10^{-20}$	2.3×10^{-19}	4.2
In#2	$(3.4 \pm 0.10) \times 10^{-20}$	1.2×10^{-19}	3.5
In#3	$(1.6 \pm 0.17) \times 10^{-21}$	4.2×10^{-21}	2.6

Consequently, PHITS overestimated for both experiments. Three possible causes of this difference were tentatively analyzed; (I) ^{7}Li(p, n) cross section, (II) Proton beam energy, and (III) Proton beam profile.

(I) ^{7}Li(p, n) cross section

Comparisons between ENDF/B-VII.0 and existing data were performed in terms of validation of ENDF/B-VII.0. **Figures 6** and **7** show ^{7}Li(p, n) cross sections and angular differential cross sections at

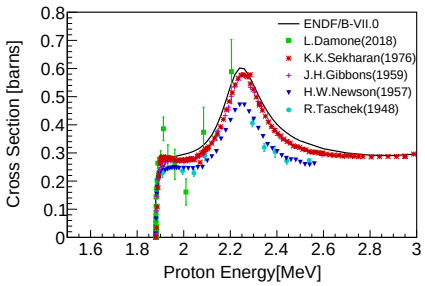

Figure 6 Comparison between ENDF/B-VII.0 and existing data cross section

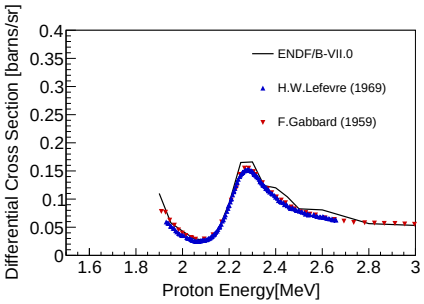

Figure 7 Comparison between PHITS with ENDF/B-VII.0 and existing data angular differential cross section (0°)

0°, respectively [2–8]. In this case, the angular differential cross sections were calculated by PHITS with ENDF/B-VII.0. Both agreed within 10 % below 2.49 MeV.

(II) Proton beam energy

Figure 8 shows the number of neutrons generated by ^{7}Li(p, n) reaction for several proton energies. When proton energy is decreased to 2.1 MeV from 2.49 MeV, neutron yields decrease about 1/4. One of the possible causes of low neutron yield in the experiment is that incident proton energy is lower than expected. It is required to measure proton energy directly.

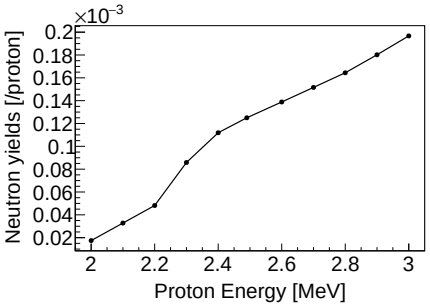

Figure 8 Neutron yields from Li target for incident proton energy

(III) Proton beam profile

Since the beam was shifted from center of the Li target in the activation experiments, it is presumed that all incident protons did not hit the Li target. In order to measure proton beam profile, an additional experiment is planned.

There are several sources of uncertainties for both experiment and calculation in the comparison process. Although one of primary uncertainty is the number of protons on the Li target during the measurement, and as it is still underway to establish a reliable diagnostics monitor system, in this study, we tentatively applied data for the number of protons based on the present system at RANS, which is obtained from current data of the whole beam pipe including the Li target. One of objectives is to confirm the total neutron yield of this particular p-Li reaction with respect to the incident proton energy. Thus, it is critical to have a correct incident proton energy. Second uncertainty source is the angular distribution of the produced neutron emitted from the Li target with respect to the proton injection direction. Third element is neutron nuclear data for the detector cross sections of both the ^{3}He(n, p) and the ^{115}In(n, n')^{115m}In reactions, and for the neutron flux spectrum simulation, which include the slowing down process in a moderator polyethylene. In addition, data associated with experimental set-up such as the distance between the Li target to the detector, weight of indium foils are important. Size of indium foil areas could matter because they are placed very near of the Li target and considerable large solid angles subtend with respect to the target center. The position of the proton beam on the target is a key to analyze the data. However, current system has a limit to identify the correct position of the proton beam. Thus we have to investigate its effect very tentatively.

5 Summary

To validate RANS-II neutron production via the ^{7}Li(p, n)^{7}Be reaction with 2.49 MeV proton injection, experiments were performed by using the long-counter using the ^{3}He counter with the polyethylene moderator and the foil activation technique for the ^{115}In(n, n')^{115m}In reaction with the 336 keV threshold energy. The reaction rates for both reactions of interest were compared with the simulation calculations by PHITS. We found that there were rather large overestimation in the calculations systematically. As the discrepancies were not able to be negligibly small, we have tried to investigate to understand possible source of the overestimation. As noted in the uncertainty section, there are many elements to arrive at the reaction rate, their contributions should be confirmed one by one. Although the process is still underway to finalize data of both experiments and calculations, In conclusion at present, the effect of proton beam shift in the Li target on the neutron flux, and the uncertainty of nuclear data for p-Li neutron production are not major source for the overestimation. This program are to be continued.

Acknowledgement

The authors would like to acknowledge the support from Neutron Beam Technology Team, RIKEN.

References

[1] Otake Y. RIKEN Compact Neutron Systems with Fast and Slow Neutrons. Plasma Fusion Res. 2018;13:2401017.

[2] Damone L, Barbagallo M, Mastromarco M, et al. ^{7}Be(n, p)^{7}Li Reaction and the Cosmological Lithium Problem: Measurement of the Cross Section in a Wide Energy Range at n_TOF at CERN. Phys Rev Lett. 2018;121(4):042701.

[3] Sekharan KK, Laumer H, Kern BD, et al. A Neutron Detector For Measurement of Total Neutron Production Cross Sections. Nucl Instrum Meth. 1976;133(2):253-257.

[4] Gibbons JH, Macklin RL. Total Neutron Yields from Light Elements under Proton and Alpha Bombardment. Phys Rev. 1959;114(2):571-580.

[5] Newson HW, Williamson RM, Jones KW, et al. Li^{7}(p, n), (p, p$'\gamma$), and (p, γ) Reactions near Neutron Threshold. Phys Rev. 1957;108(5):1294-1300.

[6] Taschek R, Hemmendinger A. Reaction Constants for Li^{7}(p, n)Be^{7}. Phys Rev. 1948;74(4):373-385.

[7] Lefevre HW, Din GU. Zero Degree Neutron Yield from the 7Li(p, n)7Be Reaction Near $2 \cdot 2$ MeV. Aust J Phys. 1969;22(6):669-678.

[8] Gabbard F, Davis RH, Bonner TW. Study of the Neutron Reactions Li^{6}(n, α)H^{3}, F^{19}(n, γ)F^{20}, and I^{127}(n, γ)I^{128}. Phys Rev. 1959;114(1):201-208.

[9] Sato T, Iwamoto Y, Hashimoto S, et al. Features of Particle and Heavy Ion Transport code System (PHITS) version 3.02. J Nucl Sci Technol. 2018;55(6):684-690.

[10] Chadwick MB, Oblozinsky P, Herman M, et al. ENDF/B-VII.0: Next Generation Evaluated Nuclear Data Library for Nuclear Science and Technology. Nucl Data Sheets. 2006;107(12):2931 – 3060.

[11] Shibata K, Iwamoto O, Nakagawa T, et al. JENDL-4.0: A New Library for Nuclear Science and Engineering. J Nucl Sci Technol. 2011;48(1):1-30.

[12] Japanese Industrial Standards Committee (JISC). Method of calibration for neutron dose equivalent (rate) meters. Japan: JISC; 2006. JIS Z 4521.

[13] Kobayashi K, Iguchi T, Iwasaki S, et al. JENDL Dosimetry File 99 (JENDL/D-99). JAERI. 2002;1344:1-133.